

---

This is an electronic reprint of the original article.  
This reprint may differ from the original in pagination and typographic detail.

Ejaz, Farhan; Kilpeläinen, Simo; Mustakallio, Panu; Zhao, Weixin; Kosonen, Risto

## **An Experimental Study on the Efficacy of Local Exhaust Systems for the Mitigation of Exhaled Contaminants in a Meeting Room**

*Published in:*  
Buildings

*DOI:*  
[10.3390/buildings14051272](https://doi.org/10.3390/buildings14051272)

Published: 01/05/2024

*Document Version*  
Publisher's PDF, also known as Version of record

*Published under the following license:*  
CC BY

*Please cite the original version:*  
Ejaz, F., Kilpeläinen, S., Mustakallio, P., Zhao, W., & Kosonen, R. (2024). An Experimental Study on the Efficacy of Local Exhaust Systems for the Mitigation of Exhaled Contaminants in a Meeting Room. *Buildings*, 14(5), Article 1272. <https://doi.org/10.3390/buildings14051272>

## Article

# An Experimental Study on the Efficacy of Local Exhaust Systems for the Mitigation of Exhaled Contaminants in a Meeting Room

Muhammad Farhan Ejaz <sup>1,\*</sup>, Simo Kilpeläinen <sup>1</sup> , Panu Mustakallio <sup>1,2</sup> , Weixin Zhao <sup>1</sup>  and Risto Kosonen <sup>1,3</sup> 

<sup>1</sup> Department of Mechanical Engineering, Aalto University, 02150 Espoo, Finland; risto.kosonen@aalto.fi (R.K.)

<sup>2</sup> Halton Oy, 00520 Helsinki, Finland

<sup>3</sup> College of Urban Construction, Nanjing Tech University, Nanjing 210037, China

\* Correspondence: muhammad.ejaz@aalto.fi

**Abstract:** In industrial applications, local exhaust systems have been used extensively for capturing and confining contaminants at their source. The present study investigates the efficacy of these systems in mitigating the spread of exhaled pollutants by combining them with mixing and displacement ventilation. Experiments were conducted in a simulated meeting room with six closely situated workstations, featuring five exposed persons (simulated with heated dummies) and one infected person (simulated with a breathing manikin). Six overhead local exhaust units, merged with panels, corresponding to workstations, were installed using a lowered false ceiling. Additionally, a table plenum setting for air inlets was introduced to enhance displacement ventilation effectiveness along with local exhaust systems. Results from 16 experimental cases are presented, using the local air quality index and ventilation effectiveness in the breathing zone. The local exhaust system improved the local air quality at the measuring locations closest to the infector in almost all test scenarios. The improvement, particularly significant with displacement ventilation, marked a maximum 35% increase in the local air quality index adjacent to the infector and 25% in the entire breathing zone of the tested meeting room. Moreover, the table plenum settings, coupled with displacement ventilation, further enhanced conditions in the breathing zone. Under the specific conditions of this investigation, the number of operational local exhausts had a marginal impact on mixing ventilation but a significant one on displacement ventilation tests. The efficacy of local exhaust systems was also influenced by the levels of heat gains present in the room. Overall, the study aims to contribute to ongoing efforts to identify sustainable solutions to mitigate indoor airborne diseases with a combination of supply and local exhaust units.

**Keywords:** local exhaust; airborne transmission; respiratory pollutants; contaminant removal; meeting room



**Citation:** Ejaz, M.F.; Kilpeläinen, S.; Mustakallio, P.; Zhao, W.; Kosonen, R. An Experimental Study on the Efficacy of Local Exhaust Systems for the Mitigation of Exhaled Contaminants in a Meeting Room. *Buildings* **2024**, *14*, 1272. <https://doi.org/10.3390/buildings14051272>

Academic Editors: Delia D'Agostino, Grzegorz Majewski, Jianbang Xiang and Shen Yang

Received: 12 March 2024

Revised: 17 April 2024

Accepted: 22 April 2024

Published: 1 May 2024



**Copyright:** © 2024 by the authors. Licensee MDPI, Basel, Switzerland. This article is an open access article distributed under the terms and conditions of the Creative Commons Attribution (CC BY) license (<https://creativecommons.org/licenses/by/4.0/>).

## 1. Introduction

In recent years, the threat of COVID-19 and other airborne diseases has caused havoc in all aspects of humanity [1]. In response to the pandemic, lockdowns were imposed to control the rapid spread of infectious diseases [2]. They proved to be effective in limiting the transmission of pathogens but they had substantial adverse impacts on economies, mental health, education sector, and overall societal well-being [3]. Thus, the situation compelled experts to explore effective mitigation strategies and fight the pandemic while keeping societies open [4].

Investigating the mechanism and characteristics of disease transmission is a prerequisite for implementing effective mitigation strategies [5]. Recent studies [6–10] have indicated that one of the primary transmission routes of COVID-19 is through the air, involving exhaled particles from infected individuals. This airborne spread encompasses various respiratory activities, including breathing, coughing, sneezing, talking, etc. Exhaled infectious particles (diameter < 100 µm) can travel room-scale distances and remain

airborne for up to hours [11–13]. These inhalable airborne contaminants have been causing cross infections, particularly in densely occupied indoor spaces such as meeting rooms, offices, or classrooms [14]. Also, in indoor settings where occupants interact closely, there is a likelihood that, intentionally or unintentionally, they may not maintain safe distances or wear masks. This increases the risk of cross-contamination in these settings [15,16]. Therefore, effective air distribution methods along with sufficient airflow rates are essential for mitigating the threat of airborne transmission in indoor settings [17–19].

Various experimental approaches, such as tracer gas measurements, aerosol particle measurements, smoke visualization, etc., along with computational fluid dynamics (CFD) studies, have been used to investigate the effectiveness of ventilation systems in reducing airborne transmission within indoor spaces [20]. Kurnitski et al. [21] introduced several ventilation designs for the post-COVID-19 era. These design methods encompass target ventilation rates and ventilation effectiveness. Their calculations were based on factors such as occupancy rates and room volumes. A CFD study [22] indicated that displacement ventilation could effectively clean the air in breathing zone by containing the heated contaminants stratified near the ceiling. Displacement ventilation can, in some cases, create a clean air layer in the occupied zone. For example, according to Sumei et al. [23] it could surpass mixing ventilation in reducing the concentration of airborne particles in the breathing zone of an office space. Some other studies [24,25] also concluded that displacement ventilation promotes vertical stratification which is effective in controlling airborne exposure in an office as compared to mixing ventilation.

However, the literature [26,27] has also highlighted the limitations of displacement ventilation, suggesting that its effectiveness in reducing airborne pathogens in the breathing zone could be contingent on factors such as location of exhausts, location of source, and size of polluted particles. Therefore, it may not be effective in all scenarios. Nielsen et al. [28] performed a tracer gas measurement for a simulated hospital ward and concluded that vertical displacement ventilation is effective in controlling cross infections but the efficiency depends on the height of return openings. Zhang et al. [29] presented an interesting observation that for short separation distances between the occupants, displacement ventilation may lead to high exposure due to thermal stratification and locking of exhaled contaminants. However, increasing separation distance reduced this effect, and eventually, displacement ventilation outperformed mixing ventilation.

Scholars have focused their efforts on personalized ventilation systems as a means of decreasing the concentration of airborne contaminants. For example, Su et al. [30] compared personalized ventilation to typical air distribution methods in a simulated office space. The investigation specified that personalized ventilation reduced infectious spread most effectively, followed by displacement ventilation, stratum ventilation, and mixing ventilation, respectively. Another study [31] indicated that, as compared to mixing ventilation, personalized ventilation could form a clean microclimate around the passenger in an aircraft cabin.

Air distribution methods such as stratum ventilation [32], impinging jet ventilation [33], and underfloor air distribution (UFAD) [34] have emerged as effective strategies to mitigate the spread of airborne contaminants in indoor environments. Similarly, air-cleaning devices have an important role in controlling the spread of airborne contaminants particularly where it is difficult to increase airflow rates or change the air distribution method. Conducted studies [35–39] have verified the usefulness of several air-cleaning methods, such as high-efficiency particulate air (HEPA) filters, ultraviolet germicidal irradiation (UVGI), and photocatalytic oxidation, in reducing the number of airborne pathogens and pollutants.

In addition to that, the literature also focuses on local exhaust methodologies to reduce airborne pollutant concentration in the breathing zone. For example, Bivolarova et al. [40] indicated that local exhaust ventilation systems could reduce pollutant exposure by up to 96% in a hospital ward. Dygert and Dang [41,42] investigated a local exhaust system with overhead and built-in-seat suction vents in a mixed indoor environment for

a simulated airplane cabin. Their CFD study with tracer gas validation determined up to a 60% decrease in co-passengers' exposure to body-emitted pollutants. Yang et al. [43] designed a personalized exhaust system for hospital consultation rooms. The effectiveness of the overhead and shoulder-mounted exhaust was tested by using a thermal manikin and tracer gas. They found that using a personalized exhaust system resulted in lower occupant exposure even after 30 min, compared to a 10 min test without the personalized exhaust system. Olmedo et al. [44] implemented a personalized exhaust system in a hospital bed and assessed its performance under various air distribution methods. They indicated that the personalized exhaust system could reduce contaminant exposure by about 57–80%. In some studies, [40,45,46], scholars also employed a combination of local exhaust and personalized ventilation to reduce contaminants in the breathing zone.

Earlier studies, including those referenced [47–54], confirm the effectiveness of face-masks in filtering respiratory particles and reducing the airborne transmission of infectious agents. However, recent investigations [52–57] have raised concerns about the discomfort, respiratory strain, and communication challenges associated with facemasks. Mask wearers often experience irritation, prompting frequent touching and adjustment, which may increase their exposure. Issues related to disturbed verbal and nonverbal communication can lead individuals to unintentionally draw closer, potentially compromising social distancing compliance. Wearing facemasks may also create a false sense of safety, reducing compliance with social distancing and handwashing guidelines. The restrictive airflow, retention, and re-inhaling of the exhaled carbon dioxide can result in hypercapnia (discomfort, muscular weakness, drowsiness, etc.) and other secondary complications. This could potentially impact productivity in office or school environments and contribute to serious health issues. Proper mask fitting is another critical factor affecting the filtration efficiency of masks. While it is challenging for the general population to achieve a secure fit, individuals with long noses or facial deformities may encounter even greater difficulties. Therefore, despite the effectiveness of using face masks, it is necessary to explore alternative and sustainable ways to combat airborne contaminants, particularly in indoor settings.

The existing literature highlights a significant research gap in assessing local exhaust systems' effectiveness in mitigating airborne spread, particularly in densely occupied indoor environments under different air distribution methods. Although existing studies report the effectiveness of local exhaust systems in environments like airplane cabins and hospitals, there is still a gap in specific research focused on densely occupied meeting rooms. The exploration of explicit indoor settings is crucial because each indoor space has unique dynamics, encompassing factors like seating arrangements, interpersonal distances, and the physical and respiratory activities of occupants. For the present study, the meeting room is being examined because it could be a focal point for cross-contamination. According to the REHVA guide [19], meeting rooms are places that are highly susceptible to cross-contamination. These spaces are common in built environments and often bustle with either long or consecutive short meetings. Moreover, they may have high occupant density, with participants engaging in more active communication compared to other working spaces such as regular offices. Therefore, precautionary measures such as wearing face masks and maintaining interpersonal distance may also be neglected.

This study aims to explore a technical solution that effectively reduces cross-contamination in indoor settings. The simulated meeting room used in the study was equipped with a local exhaust system. A combination of local exhaust with either displacement or mixing air distribution methods is examined. In addition to that, a method to enhance the performance of displacement ventilation using a table plenum setup is analyzed. It also explores the effect of heat gains experienced by indoor environments during a typical summer and mid-season. Moreover, the influence of the number of operational local exhausts in the occupied zone is considered. The findings of the study provide valuable insights to reduce airborne contagions and improve occupant well-being in densely occupied indoor spaces.

## 2. Materials and Methods

### 2.1. Experimental Setup

#### 2.1.1. Test Chamber

Experimental measurements were conducted in a full-scale test room, as depicted in Figure 1, where indoor conditions were kept at a steady state. The test room had dimensions of 5.50 m (L), 3.84 m (W) and 3.60 m (H). It was situated within a laboratory hall which ensured a stable external environment around the test chamber. The test chamber was employed to simulate a meeting room with six closely spaced workstations.

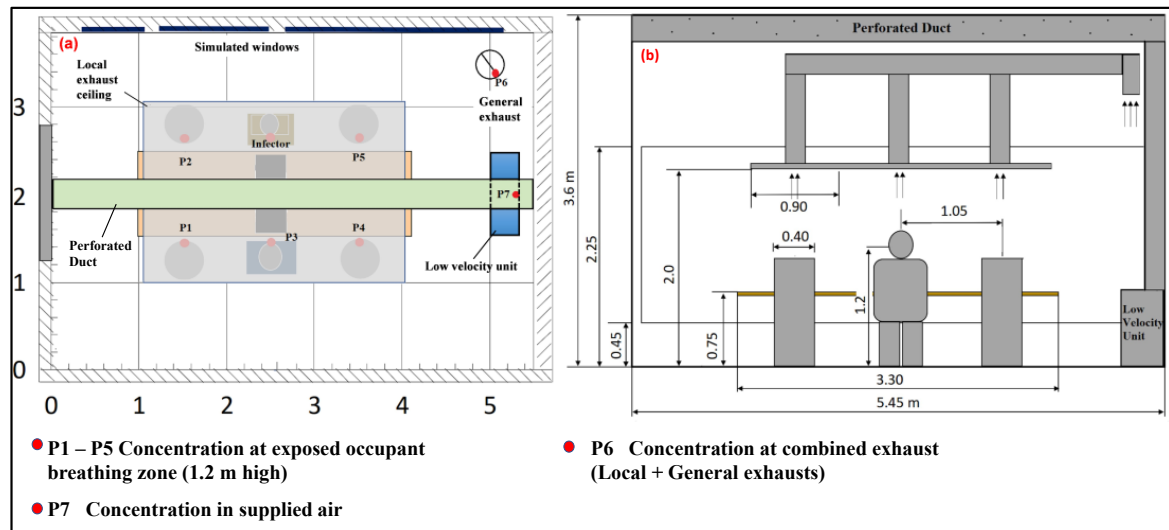
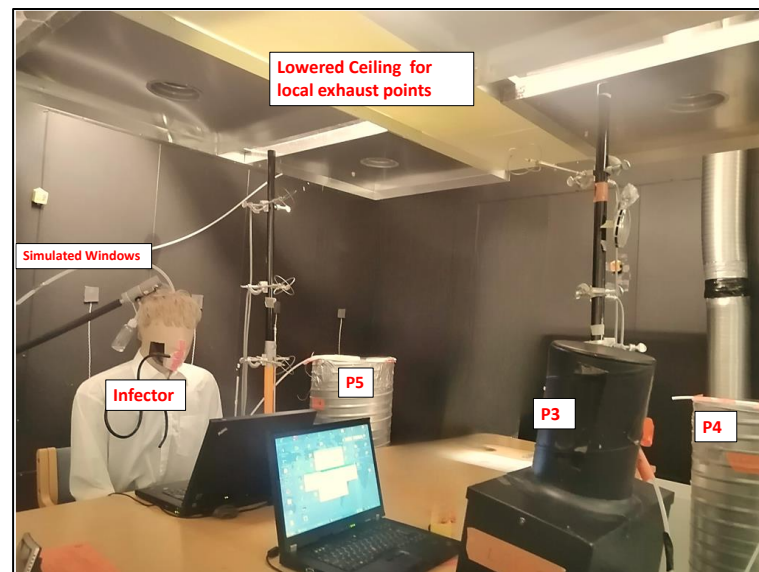


Figure 1. The layout of the test chamber: (a) top view (b) side view.

The workstations had one thermal breathing manikin (PT: Teknik, Hillerød, Denmark) as the infector and five heated dummies representing the exposed occupants, as illustrated in Figure 2. At location P3 (Figures 1a and 2), a heated dummy was present that imitated a human with body parts like head, chest, and legs. The dummy consisted of 75-watt heating elements distributed among the body parts. The remaining four dummies (P1, P4, P5, and P6) were cylindrical, measuring 0.8 m in diameter and 1.2 m in length. They were also equipped with 75-watt heating elements to simulate the direct solar gain along the length. Temperature of around 34–36 °C, which matches that of a normal human. The heat gain varied between 75 and 85 W/m<sup>2</sup> with an approximate average of 80 W/m<sup>2</sup>. A lowered ceiling with six local exhaust units, each corresponding to a workstation, was installed. These exhaust units were merged seamlessly, forming a panel with no cracks between them. Two laptops were also present at the workstations, and light bulbs were installed above the local exhaust ceiling. The local exhaust false ceiling was metallic with some transparent glass sections that allowed light from the bulb to reach the occupied zone. Solar heat gain through windows was simulated using heated panels on one of the walls (Figure 2) where the surface temperature could be controlled. An electric heating foil (5.0 m × 1.0 m) was located under the workstations to simulate the direct solar radiation on the floor. The sources of two different heat gain levels used in this study for the space under consideration are summarized in Table 1. The indoor temperature for all tests was maintained at 25 ± 1 °C. Heat gains were balanced by increasing the supply airflow rates to maintain the set target temperature, as described in subsequent sections.





**Figure 2.** Experimental arrangement.

The floor area of the two different heat gain levels used in this study for the space under consideration are summarized in Table 1. The indoor temperature for all tests was maintained at  $25 \pm 1$  °C. Heat gains were balanced by increasing the supply airflow rates to maintain the set target temperature, as described in subsequent sections.

| Sources of Heat Gain (W)             | Heat Gains (W) | Heat Gains ( $W/m^2$ ) |
|--------------------------------------|----------------|------------------------|
| Manikin                              | 80 W           | 80 W                   |
| Equipment (75 × 50 cm)               | 375 W          | 375 W                  |
| Laptops (40 × 2 pc)                  | 80 W           | 80 W                   |
| Ceiling light                        | 90 W           | 90 W                   |
| Simulated solar gain from windows    | 643 W          | 33.2 ( $W/m^2$ )       |
| Simulated direct solar gain at floor | 420 W          | 0 W                    |
| Equipment (manikin's controllers)    | 50 W           | 50 W                   |
| Total heat gain                      | 1330 W         | 700 W                  |

2.1.2. Ventilation System. In this study, local exhaust systems were employed and evaluated with two different air distribution methods. The aim was to assess their effectiveness in mitigating the spread of exhaled airborne contaminants. Tests were conducted separately for mixing and displacement air distribution systems. The mixing system supplied air through a perforated duct that was installed in the middle of the ceiling at 3.25 m height as illustrated in Figure 1.

The length of the perforated duct was 5.5 m, and the diameter was 200 mm. In displacement ventilation, the air was supplied through a low-velocity unit placed on the floor at the back of the room beside the wall (Figure 1). The unit supplied air in the longitudinal direction beneath the table towards the workstations.

The local exhaust hoods were installed on the ceiling at 3.25 m height as illustrated in Figure 1. The length of the perforated duct was 5.5 m, and the diameter was 200 mm. For displacement ventilation, the air was supplied through a low-velocity unit placed on the floor at the back of the room beside the wall (Figure 1). The unit supplied air in the longitudinal direction beneath the table towards the workstations. The supply air velocity at the workstation was adjusted to be 10 L/s. All exhaust hoods were connected to the ceiling using a suspended ductwork ceiling duct to the main duct (3 m × 2 m) general exhaust grille merged with plates, and installed in the ceiling (Figure 1).

Equipment with the adjustable lamping and displacement ventilation chamber to take equipment. The local exhaust effect of local exhaust system was adjusted to be useful design exhaust point with the displacement method. The displacement to the local positions, adjacent to the working table height of 3 m, was installed at the table to be (Figure 1).

In addition to the conventional mixing and displacement ventilation, this study also examines the combined mitigating effect of local exhaust systems and a table plenum design in conjunction with the displacement air distribution method. The displacement unit was positioned adjacent to the working table, which supplied air beneath the table. To enhance its effectiveness, the table plenum settings, as depicted in Figure 3, were implemented by adding partition curtains (walls) to enclose the space under the table with openings near the occupants.

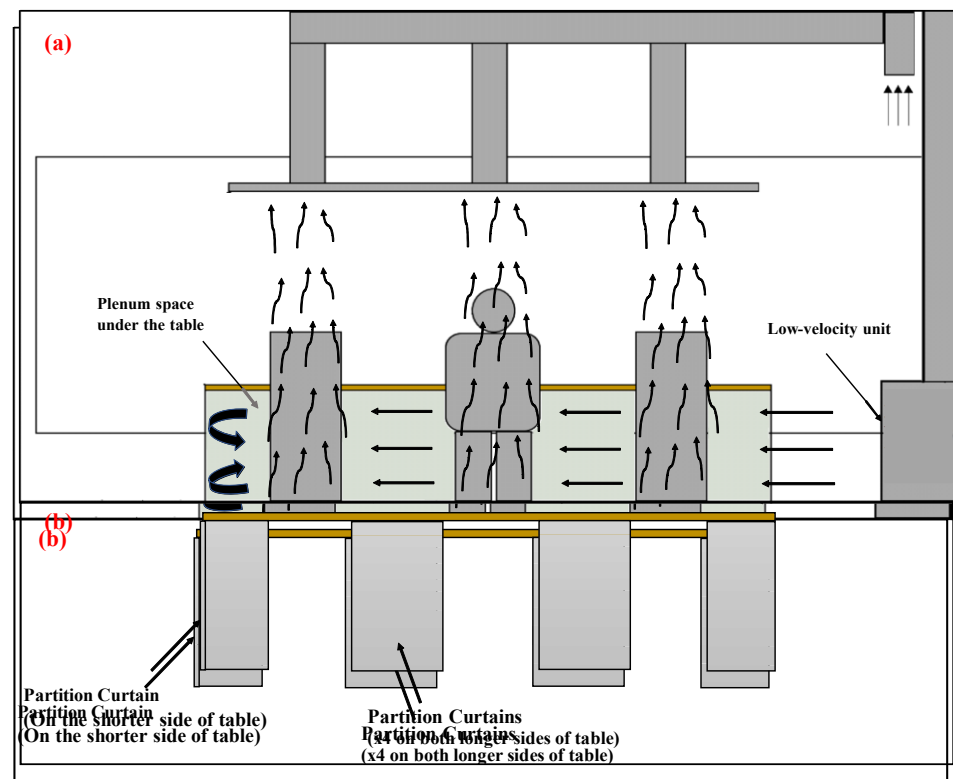


Figure 3. Table plenum design: (a) side view; (b) table plenum configuration.

The supply air openings for the table plenum are depicted in Figure 4. The green arrows represent the location of air openings and the corresponding airflow direction from these openings. The air, including pollutants, rises through these openings propelled by convective flows generated by simulated persons and is subsequently captured by overhead local exhausts.

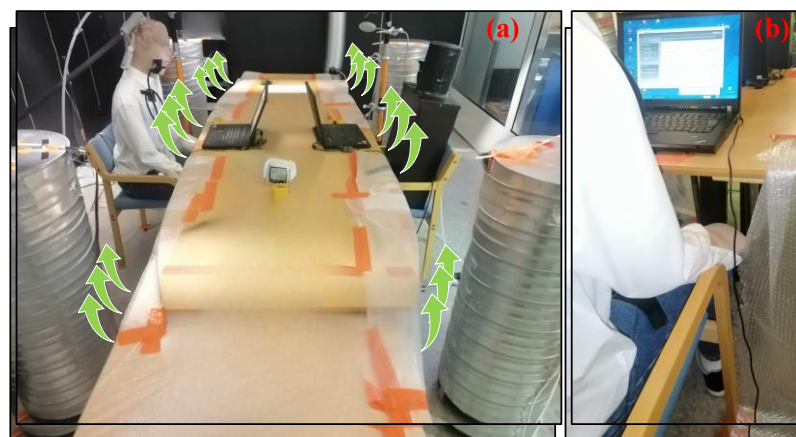


Figure 4. Supply air openings with table plenum: (a) all openings; (b) close-up for infector's opening.

### 2.1.3. Thermal Breathing Manikin

The thermal breathing manikin comprised 27 heated body segments and was utilized to simulate an infected person in a seated position with an average heat gain of 80 watts. The manikin's dimensions replicated a 1.75 m tall male. The temperature and heating power of the body segments could be controlled by a computer program. Throughout the

experiments, the surface temperature of the manikin was regulated to approximate the skin temperature of an occupant experiencing thermal comfort in a controlled environment (34–36 °C). The manikin was dressed in a short-haired wig, vest, shirt, trousers, light socks, and light shoes, thereby simulating typical office attire for the summer season, with a thermal insulation rating of 0.5 clo. The nostrils of the manikin were shaped as round openings with an area of 44.2 mm<sup>2</sup> each, and the mouth had the form of an ellipsoidal opening with an area of 113.4 mm<sup>2</sup>. The two jets from the nostrils were deflected 45° downwards from the horizontal axis.

To simulate real human breathing, the manikin was connected to an artificial lung, enabling control of breathing patterns. In this study, the manikin inhaled by mouth and exhaled by nose. The designed pulmonary ventilation rate was 6.0 L/min [58]. Each breathing cycle consisted of 2.5 s of inhalation, 1.0 s break, 2.5 s exhalation, and 1.0 s break. The exhaled air mixed with the tracer gas from the manikin was heated to 35 °C and humidified to about 85% RH. Tracer gas was injected directly into the artificial lung of the infector. The rate of the tracer gas dose was 2.5 mL/min and the pulmonary ventilation rate of the infector was 6 L/min which is the normal breathing rate of a male adult at rest [58]. Therefore, the tracer gas concentration in the exhaled air of the infector was approximately 20,000 ppm.

#### 2.1.4. Measured Parameters and Instrumentation

For this investigation, we deliberately chose sulfur hexafluoride (SF<sub>6</sub>) as the tracer gas after comparing its characteristics with alternatives like carbon dioxide (CO<sub>2</sub>) and nitrous oxide (N<sub>2</sub>O). SF<sub>6</sub> was preferred because it is not usually found in the outdoor air and can be detected even at very low concentrations. It is typically odorless, chemically inert, and safe at the concentration level used in the present investigation. However, both N<sub>2</sub>O and CO<sub>2</sub>, which have a relatively similar density to air, are normally a constituent of air and tend to mix and disperse quicker than SF<sub>6</sub>. These characteristics of N<sub>2</sub>O and CO<sub>2</sub> may potentially impact the accuracy of measurements in specific experimental conditions of this study. Moreover, SF<sub>6</sub> has also been used by scholars in similar studies such as [42,59–61].

A multi-gas analyzer platform (GASERA one, Turku, Finland), with an accuracy of approximately 0.5 ppm, conducted continuous tracer gas measurements. These measurements were performed at seven locations (P1–P7), as illustrated in Figure 1. Points P1 to P5 were situated at the exposed occupant's mouth height (1.2 m) and measured tracer gas inhalable concentration. P6 was at the combined exhaust point just before the final air extraction from the room. While P7 provides information about the contaminant concentration at either mixing or displacement supplied air close to the terminal unit.

#### 2.2. Experimental Process and Scenarios

The measurement process started by adjusting the total supply airflow rate and exhaust flow rates according to heat gains and air conditioning requirements. Each operational local exhaust flow was set to 10 L/s. The flow rate of the general exhaust varied depending on the experimental scenario. A multifunction meter (TSI, Aachen, Germany, TC9650) equipped with a hot wire anemometer probe (TSI, Aachen, Germany, TC966) was used for velocity measurements at the exhaust points. A large rectangular volume flow hood was then employed to calculate volume flow from velocity measurements. This flow measurement process maintained the overall balance of the system with minimum disturbance. The adjustable damper installed at each exhaust point was then used to adjust the required exhaust flow. A smoke test was conducted to visualize and ensure proper air movement and functionality of the exhaust points. Then, tracer gas dosing was initiated after the indoor airflow distribution and room conditions had reached steady-state conditions, a process that typically took about 1 h. Then, a continuous measurement of tracer gas concentration at all measuring locations P1 to P7 (Figure 1) was conducted throughout the test.

The supply airflows were 116 L/s and 61 L/s for the 64 W/m<sup>2</sup> and 33.2 W/m<sup>2</sup> heat gain levels, respectively. This resulted in specific airflow rates of 5.5 1/(s, m<sup>2</sup>) and



2.9 l/(s, m<sup>2</sup>). The reference air temperature (accuracy of  $\pm 0.2$  °C) was kept at  $25 \pm 1$  °C at measured at the heights of 1.1, 1.5, and 1.9 m. The supply air temperature for all experiments was 16 °C. The relative humidity of the indoor air was not actively controlled, and it varied slightly between 30% and 40% during the experiments. A description of test scenarios is presented in Table 2.

**Table 2.** Description of test scenarios.

| Case | Heat Gain             | Air Distribution System   | No. of Local Exhaust | Exhaust Flow Rates        |                 |
|------|-----------------------|---|----------------------|---------------------------|-----------------|
|      |                       |   |                      | Local Exhausts            | General Exhaust |
| 1    | 33.2 W/m <sup>2</sup> | Mixing<br>(61 L/s $\pm$ 5%, 25 $\pm$ 1 °C)                          | 0 (Reference Case)   | 0 L/s                     | ~61 L/s         |
| 2    |                       |   | 2                    | 20 L/s: 2 $\times$ 10 L/s | ~41 L/s         |
| 3    |                       |   | 6                    | 60 L/s: 6 $\times$ 10 L/s | ~0~1 L/s        |
| 4    |                       | Displacement<br>(61 L/s $\pm$ 5%, 25 $\pm$ 1 °C)                    | 0 (Reference Case)   | 0 L/s                     | ~61 L/s         |
| 5    |                       |   | 2                    | 20 L/s: 2 $\times$ 10 L/s | ~41 L/s         |
| 6    |                       |   | 6                    | 60 L/s: 6 $\times$ 10 L/s | ~0~1 L/s        |
| 7    | 64 W/m <sup>2</sup>   | Displacement with table plenum<br>(61 L/s $\pm$ 5%, 25 $\pm$ 1 °C)  | 2                    | 20 L/s: 2 $\times$ 10 L/s | ~41 L/s         |
| 8    |                       |   | 6                    | 60 L/s: 6 $\times$ 10 L/s | ~0~1 L/s        |
| 9    |                       | Mixing<br>(116 L/s $\pm$ 5%, 25 $\pm$ 1 °C)                         | 0 (Reference Case)   | 0 L/s                     | ~116 L/s        |
| 10   |                       |   | 2                    | 20 L/s: 2 $\times$ 10 L/s | ~96 L/s         |
| 11   |                       |   | 6                    | 60 L/s: 6 $\times$ 10 L/s | ~56 L/s         |
| 12   |                       | Displacement<br>(116 L/s $\pm$ 5%, 25 $\pm$ 1 °C)                   | 0 (Reference Case)   | 0 L/s                     | ~116 L/s        |
| 13   |                       |   | 2                    | 20 L/s: 2 $\times$ 10 L/s | ~96 L/s         |
| 14   |                       |   | 6                    | 60 L/s: 6 $\times$ 10 L/s | ~56 L/s         |
| 15   |                       | Displacement with table plenum<br>(116 L/s $\pm$ 5%, 25 $\pm$ 1 °C) | 2                    | 20 L/s: 2 $\times$ 10 L/s | ~96 L/s         |
| 16   |                       |   | 6                    | 60 L/s: 6 $\times$ 10 L/s | ~56 L/s         |

### 2.3. Evaluation Indices

For this study, the performance is analyzed with the local air quality index ( $\varepsilon_p$ ), a methodology subsequently adopted by earlier studies, including [21,42]. The index provides local air quality information about the specific measurement point. It is calculated as follows:

$$\varepsilon_p = \frac{C_e - C_s}{C_p - C_s} \quad (1)$$

where

$C_e$  is the contaminant concentration in the combined exhaust duct;

$C_p$  is the contaminant concentration at the concerned measuring location (P1–P5);

$C_s$  is the contaminant concentration in supply air ( $C_s \approx 0$  for all the measured cases).

Ventilation effectiveness ( $\varepsilon_v$ ) is defined in REHVA Guidebook no. 2 [62] as the following:

$$\varepsilon_v = \frac{C_e - C_s}{C_i - C_s} \quad (2)$$

For this study, point source ventilation effectiveness for breathing zone  $\varepsilon_v^b$  is calculated as reported by Kurnitski et al. [21]. Unlike the local air quality index which offers information specific to individual measurement points,  $\varepsilon_v^b$  provides insights into the air quality across the entire breathing zone within the investigated meeting room. It is calculated as follows:

$$\varepsilon_v^b = \frac{C_e - C_s}{C_b - C_s} \quad (3)$$

lated as follows:

$$\varepsilon_v^b = \frac{C_e - C_s}{C_b - C_s} \quad (3)$$

where

$C_i$  is the averaged contaminant concentration in the room.

where  $C_b$  represents the averaged contaminant at the breathing zone level and is calculated using the following formula:

$C_b$  represents the averaged contaminant at the breathing zone level and is calculated using the following formula:

$$C_b = \frac{\sum_{Pi=1}^{Ph=5} C_i}{n = 5} \quad (4)$$

In determining  $C_b$ , Kurnitski et al. [21] used a 50% measurement points rule, calculating the average concentration from 50% of the measurement points with the highest concentrations. However, in the present study, all five measurement points were averaged due to the limited number of points, and for mixing ventilation, concentrations at measuring points exhibited considerable similarity. However, in the present study, all five measurement points were averaged due to the limited number of points, and for mixing ventilation, concentrations at measuring points exhibited considerable similarity.

### 3. Results

#### 3.1. Assumption of Steady State

##### 3.1.1. Assumption of Steady State

Two indices,  $\varepsilon_p$  and  $\varepsilon_v^b$ , used for the evaluation of measurements, are deemed valid when the contaminant concentrations in the indoor environment attain a steady state. For this investigation, a steady state is assumed when the contaminant concentration in the combined exhaust stabilized during the three-hour tests. One of the cases, as depicted in Figure 5, shows how the concentration stabilizes in the last two hours after initially rising for an hour following the start of contaminant injection at a time of 0 min.

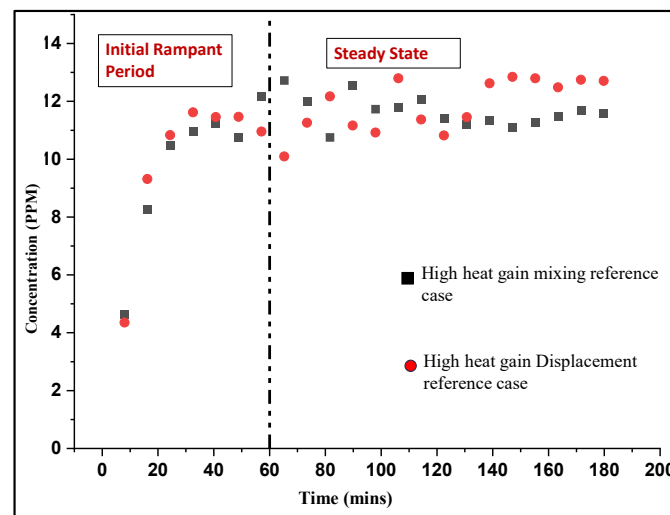


Figure 5. Exhaust concentration for high heat gain reference cases.

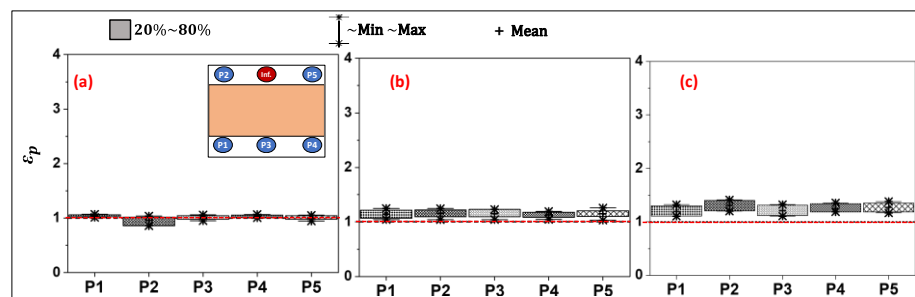
##### 3.2. Local Air Quality Index ( $\varepsilon_p$ )

The local air quality index ( $\varepsilon_p$ ) measures the effectiveness of ventilation systems in removing contaminants from the immediate vicinity of measurement points, i.e., the simulated individuals. Box plots are used to summarize the variation in the  $\varepsilon_p$  in the breathing zones of occupants at locations P1 to P5. The box indicates the primary data range between the 20th and 80th percentiles. The whiskers extending from the box show the dataset's minimum and maximum values. Also, a red dotted line is consistently used to signal a critical threshold; a maximum value of 1. A concentration below this line indicates that the pollutant concentration at the specific measurement point is higher compared to the concentration in the exhaust duct. In other words, poor air quality conditions occur when  $\varepsilon_p < 1$ .

Figure 6a indicates that in the reference test of the mixing system with low heat gain ( $33.2 \text{ W/m}^2$ ), the local air quality index  $\varepsilon_p$  values for locations P2 and P5 were not only less

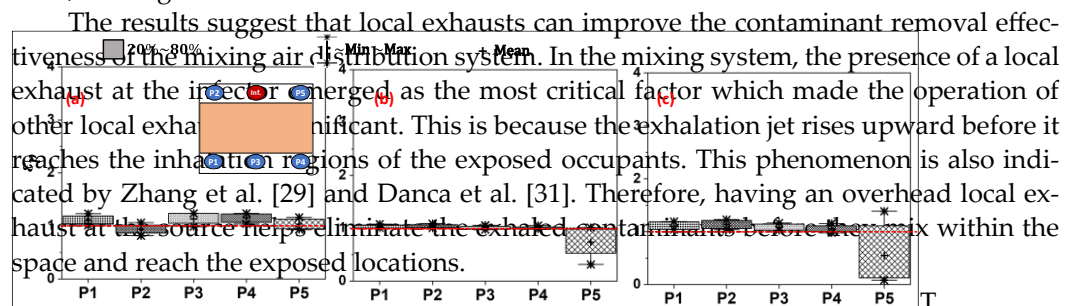
icates that the pollutant concentration at the specific measurement point is higher compared to the concentration in the exhaust duct. In other words, poor air quality conditions occur when  $\varepsilon_p < 1$ .

Figure 6a indicates that in the reference test of the mixing system with low heat gain (33.2 W/m<sup>2</sup>), the local air quality index  $\varepsilon_p$  values for locations P2 and P5 were not only less than the critical value of 1 but also lower than the values observed at the other measurement points. This suggests that the exhaled airflow from the infector's nose predominantly spreads sideways, affecting the locations adjacent to the infector. The introduction of local exhausts, as shown in Figure 6b, apparently improved the air quality situation at local exhausts P2 and P5 but also enhanced the conditions at other measurement points. Figure 6b also indicates that the feeding of the improved air quality at all measuring points with  $\varepsilon_p$  almost exceeding the critical value of 1. A significant increase in air quality at measurement points was approximately 15% critical compared to the reference case. The significant increase was observed at the approximately adjacent to the infector for the P2 (reference case) and observed at the adjacent to the infector for P2 (reference case) and observed at the adjacent to the infector for P2 (reference case). Additionally, there was an approximately 10% increase in  $\varepsilon_p$  at P3 (reference case) and P4 (reference case) from the infector, i.e., P1 ( $\varepsilon_p \approx 1.25$ ), P3 ( $\varepsilon_p \approx 1.2$ ) and P4 ( $\varepsilon_p \approx 1.3$ ).



**Figure 6.** Local air quality ( $\varepsilon_p$ ) at the breathing zones (P1–P5) for low heat gain mixing distribution cases. (a) Reference case (no local exhausts), (b) Two operational local exhausts (at infector and location P3), (c) Six operational local exhausts.

The results of the test scenarios for mixing gases with high heat gain (64 W/m<sup>2</sup>) are summarized in Figure 7a–c. The introduction of local exhausts either two or six led to slight improvement at locations P1 to P4, while P5 experienced deterioration in this case and  $\varepsilon_p$  not only reduced but also fell below the critical value of 1. Under high heat gain conditions, a higher supply airflow rate of 116 L/s was employed to balance heat gains and maintain the room temperature at 25 °C. Consequently, the flow rate of the general exhaust was set at 96 L/s for scenarios involving two operational local exhaust points and 56 L/s for cases with six operational local exhaust points, as the operational local exhaust flow rate remained constant at 10 L/s throughout. Location P5 was between this high-flow general exhaust point, the lowered suspended ceiling, and the neighboring infector. The combination of these factors overcame the local exhaust effect (10 L/s) at location P5, and the high-flow general exhaust pulled the exhaled jet from the infector manikin towards itself, making P5 a vulnerable location.



**Figure 7.** Local air quality ( $\varepsilon_p$ ) at the breathing zones (P1–P5) for high heat gain mixing distribution cases. (a) Reference case (no local exhausts), (b) Two operational local exhausts (at infector and location P3), (c) Six operational local exhausts.

The results suggest that local exhausts can improve the contaminant removal effectiveness of the mixing air distribution system. In the mixing system, the presence of a local exhaust at the infector emerged as the most critical factor which made the operation of other local exhausts significant. This is because the exhalation jet rises upward before it reaches the inhalation regions of the exposed occupants. This phenomenon is also indicated by Zhang et al. [29] and Danca et al. [31]. Therefore, having an overhead local exhaust at the source helps eliminate the exhaled contaminants before they mix within the space and reach the exposed locations.

On the other hand, for low heat gain, displacement air distribution, as shown in Figure 8a–e, ensured a cleaner breathing zone at all exposed locations. Figure 8a exhibits that for the reference case of displacement ventilation at low heat gain ( $33.2 \text{ W/m}^2$ ),  $\varepsilon_p > 1$  for all measured locations. Like the mixing test cases, the adjacent locations P2 and P5 were comparatively more exposed than others. However, the extent of exposure was smaller than in the corresponding mixing ventilation tests. With the introduction of a local exhaust to reach the contamination regions of the exposed occupants, this phenomenon is also indicated by Zhang et al. [29] and Dima et al. [31]. Therefore, having an overhead local exhaust at the source helps eliminate the exhaled contaminants before they mix within the space and reach the exposed locations.

On the other hand, for low heat gain, displacement air distribution, as shown in Figure 8a, local air quality index ( $\varepsilon_p$ ) at each measuring location. A substantial increase of at least 35% was reported at location P3 when compared to cases without any local exhaust (reference case). At locations P1, there was an increase of about 15%. Locations P2 and P5 roughly 25% increase in more exposed than others, the measuring locations specifically at P1 (from 1.9 to 2.9), P3 (from 2.0 to 2.9), and P4 (from 2.0 to 2.9) in the ventilation tests. With the introduction of a local exhaust to displacement ventilation, by using a table plenum, the situation exhausts measuring location became better. The sideways spread of contaminants was successfully reduced by total exhaust systems at locations where local exhausts were active. Therefore, six operational local exhausts as illustrated in Figure 8d, the result indicates a significant increase in local air quality index ( $\varepsilon_p$ ) at each measuring location. A substantial increase of at least 35% was reported at location P3 when compared to cases without any local exhaust (reference case). At location P1, there was an increase of about 15%. There was also a roughly 25% increase in mean values and a further enhanced the air quality at locations (P1 and P2) situated farthest from the source of supply air.

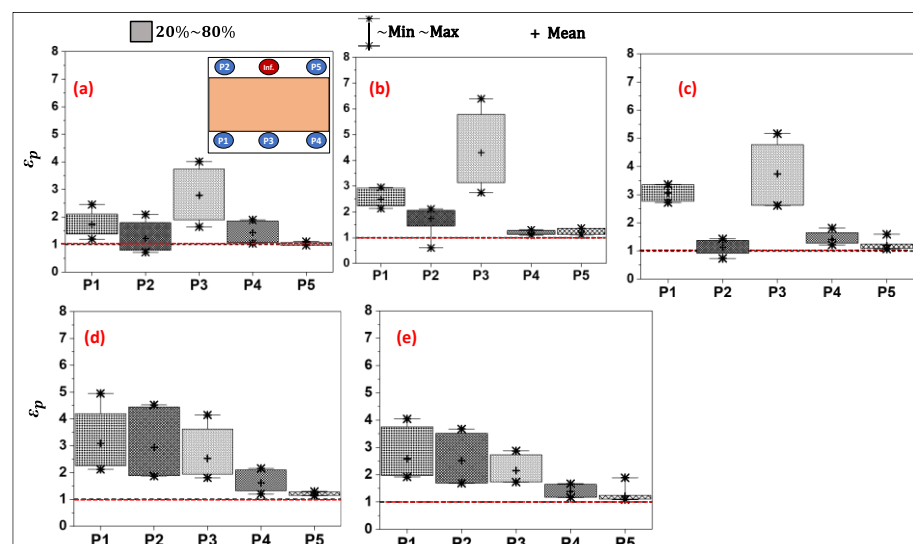


**Figure 8.** Local air quality ( $\varepsilon_p$ ) at the breathing zones (P1–P5) for low heat gain displacement distribution cases. (a) Reference case (no local exhaust). (b) Two operational local exhausts (at infector and location P3). (c) Two operational local exhausts with table plenum. (d) Six operational local exhausts. (e) Six operational local exhausts with table plenum.

However Figure 8a,b,d suggest that the number of local exhausts also has a substantial impact in displacement cases. The air quality is better and contaminant removal is more significant at locations where local exhausts were active. Therefore, a local exhaust system with six operational exhausts is more effective than the system with two operational local exhausts and displacement ventilation.

The effect of the table plenum for two and six operational local exhausts for low heat gain is presented in Figure 8c,e. This setting improved the delivery of supply air close to the occupants and it enhanced the air quality at locations (P1 and P2) situated farthest from the source of supply air.

The effect of local exhausts for the high heat gain displacement air distribution case is illustrated in Figure 9a–e. In contrast to the previously discussed cases, the reference case, as illustrated in Figure 9a, demonstrated less lateral spread of contaminants towards P2 and



ical value of 1. The effect of the number of local exhausts was also present in high heat gain cases and air quality was relatively better at locations where local exhausts were operational.

At high heat gain when there was a higher supply airflow rate, the influence of the table plenum became more prominent, particularly in the case with six exhaust points. The table plenum provided a designated path for supplying air to the farthest locations from the supply air terminal, namely P1, and P2, resulting in a minimum 15% increase in  $\epsilon_p$ . This is due to the relatively high locations. Also, this table plenum is setting the delivery rate of the supply air flow among all occupants with a single supply inlet. Figure 9 suggests that the local exhausts supplied heat load and the introduction of local exhausts (Figure 9b,d) led to the effect of location and being placed is likely higher exhaust flow rate to the lower ceiling and in the corner of the room still existed, but it did not fall below the critical value of 0.5. The effect of the number of local exhaust settings also present in high heat gain cases and air quality was relatively better at locations where local exhausts (Figure 9e) were operational.

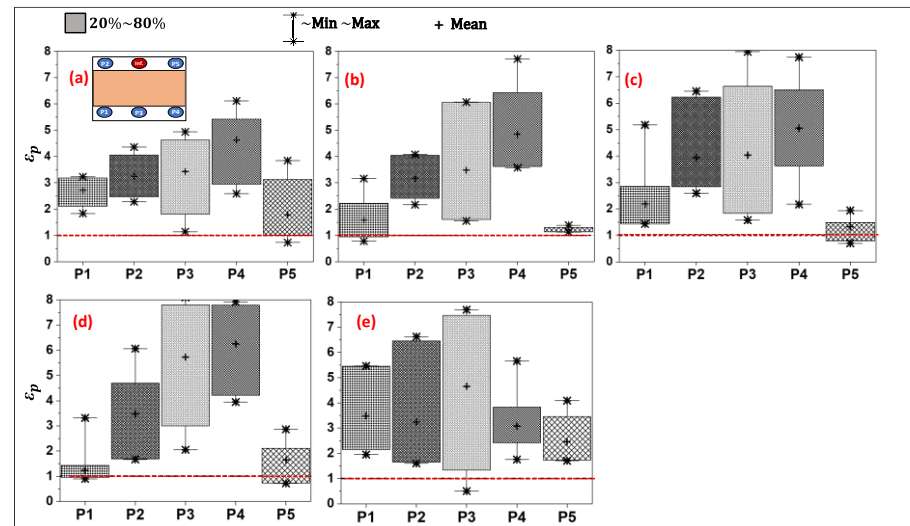


**Figure 9.** Local air quality ( $\epsilon_p$ ) at the breathing zone (P1–P5) for high heat gain displacement distribution cases: (a) Reference case (no local exhausts); (b) Two operational local exhausts (at infector and location P3); (c) Two operational local exhausts with table plenum; (d) Six operational local exhausts; (e) Six operational local exhausts with table plenum.

The results indicate that local exhaust systems perform better with displacement air distribution compared to mixing systems. A significant reduction in exhaled contaminants was observed at measured locations, particularly close to the infector. This is because displacement air distribution systems introduce outdoor air at low height, and gradually push it upwards to carry contaminants away from occupants. Also, the table plenum setting provided a more balanced supply airflow among all occupants with a single supply inlet.

Also, in the case of high heat load, the introduction of local exhausts (Figure 9b,d) led to a decrease in air quality at P1. This is likely because the local exhausts may have extracted some of the clean outdoor air before it reached P1. This phenomenon was also mitigated by utilizing table plenum settings. Consequently, table plenum resulted in a more uniform and better air quality at all locations (Figure 9e).

The results indicate that local exhaust systems perform better with displacement air distribution compared to mixing systems. A significant reduction in exhaled contaminants was observed at measured locations, particularly close to the infector. This is because displacement air distribution systems introduce outdoor air at low height, and gradually push it upwards to carry contaminants away from occupants. The upward airflow characteristic of displacement systems aligns well with the vertical extraction of overhead exhaust points. The effect of the number of operational local exhausts is prominent in displacement cases. Earlier studies [31,63] have reported that in displacement air distribution, contaminants can travel significant distances horizontally because of a lock-up effect of exhaled contaminants at the breathing zone. Therefore, it is important to have local exhausts at other locations in addition to the contamination sources. The table plenum with displacement ventilation further increases local air quality as it provides a designated path to supply uniform air to all the occupants.

was seen in the case of six local exhausts. However, with the displacement system at low heat gain, the  $\varepsilon_v^b$  value approached 1.7 for two operational local exhausts representing an increase of approximately 15% compared to its reference case. This value further increased to 2 with 6 operational local exhausts, marking a 22% increase in ventilation effectiveness for the breathing zone. The table plenum further enhanced displacement air distribution by increasing  $\varepsilon_v^b$  by about 5% compared to scenarios where it was not employed.

At high heat gain, the local exhaust with mixing air distribution system slightly compromised the overall air quality. This was primarily due to elevated contaminant concentrations at location P5, influenced by a lower ceiling and its positioning in the path of contaminant flow toward a high-flow-rate general exhaust. The  $\varepsilon_v^b$  value decreased by about 16% (as compared to high heat gain mixing reference case) for both two and six operational local exhausts. However, with displacement ventilation, the value of  $\varepsilon_v^b$  which approached 2.75, indicating a 19% increase for 2 local exhausts. When utilizing 6 local exhausts,  $\varepsilon_v^b$  approached 3 which is about 25% higher as compared to the high heat gain displacement reference case. The impact of the table plenum was particularly important in the high heat gain system when combined with six local exhausts. This combination significantly improved the performance of displacement air distribution, demonstrating an increase of approximately 12% compared to cases where the table plenum was not utilized. Increasing  $\varepsilon_v^b$  by about 5% compared to scenarios where it was not employed.

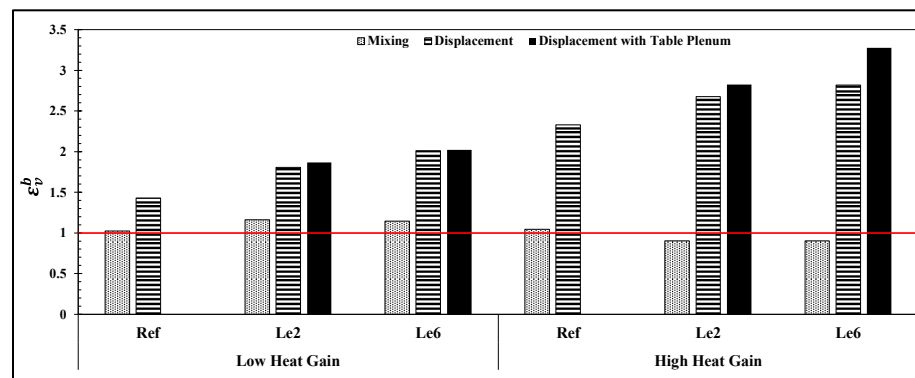


**Figure 10.** Point source ventilation effectiveness for the entire breathing zone.

At high heat gain, the local exhaust with mixing air distribution system slightly compromised the overall air quality. This was primarily due to elevated contaminant concentrations at location P5, influenced by a lower ceiling and its positioning in the path of contaminant flow toward a high-flow-rate general exhaust. The  $\varepsilon_v^b$  value decreased by about 16% (as compared to high heat gain mixing reference case) for both two and six operational local exhausts. However, with displacement ventilation, the value of  $\varepsilon_v^b$  approached 2.75, indicating a 19% increase for 2 local exhausts. When utilizing 6 local exhausts,  $\varepsilon_v^b$  approached 3 which is about 25% higher as compared to the high heat gain displacement reference case. The impact of the table plenum was particularly important in the high heat gain system when combined with six local exhausts. This combination significantly improved the performance of displacement air distribution, demonstrating an increase of approximately 12% compared to cases where the table plenum was not utilized.

#### 4. Discussion

The experimental findings of the present study confirm that local exhaust systems effectively enhance conventional air distribution systems in reducing the airborne spread of exhaled contaminants. However, their impact depends on factors such as the air distribution method, location and strength of heat gains, and the number of operational local exhausts. Earlier studies [41,42,44] have indicated similar observations in other indoor spaces. Scholars [41,42] achieved a minimum 30% reduction in exposure by testing overhead, seat, and window-mounted local exhausts in a mixed-air cabin. Their exhaust flow rate varied between 7 and 15 L/s. Olmedo et al. [44] implemented a personalized exhaust system on the patient's bed near to its head in a hospital ward. They achieved a minimum of 57% efficiency with about 50 L/s exhaust flow rate. However, such settings with closer exhaust points and higher flow rates are not feasible in a meeting room space due to more active communication and occupant movement.

The local exhaust systems utilized in the presented study do not disturb the workspace of occupants. Also, they are easy to install in existing building stock and do not add any

extra energy costs to the system. The local exhaust functions like a point sink and sucks air from its surroundings. The suction velocity decreases proportionally to the square of the distance from the exhaust face. This feature is well known in studies of local exhaust ventilation, particularly in industrial settings. The implication of this phenomenon has both advantages and disadvantages. On the positive side, it reduces discomfort for occupants by avoiding strong airflows. But, it limits the system's ability to capture contaminants effectively. However, the potential comfort issues associated with local exhausts operating at higher flow rates are the acoustic problems that may affect the occupants [42,64,65].

In this study, ventilation effectiveness (contaminant removal effectiveness) serves as the primary evaluation index. This index has been extensively utilized in previous studies (e.g., in [60,62,66]), and it offers a reliable, quick, and straightforward prediction of pathogen spread and comparison both in experiments and numerical simulations. The usefulness of the index comes from its ability to directly show the situation compared to threshold value (typically 1) in a fully mixed environment. However, it falls short of assessing the infectivity of specific disease agents. Also, this index is relative and normalized with the pollutant's concentration at the exhaust. That is why if not used carefully, it may potentially lead to false conclusions about the absolute concentration of contaminants in the indoor environment.

The present study primarily evaluates the effect of air distribution systems on contaminant concentration, which is why the tracer gas method was used. A potential future direction regarding various other experimental methods could involve using microorganisms instead of tracer gas. Microorganisms may offer a direct representation of airborne pathogens but also pose challenges like feasibility, maintenance, and safety. Biological pollutants might be more helpful when the primary goal is to evaluate disinfection methods such as UV lights, ozone generators chemical disinfectants, and other similar methods. Moreover, particle-based aerosols are useful when evaluating filtration techniques or studying the deposition of infectious particles [35,67].

This study's results encourage further exploration of local exhausts, particularly in the context of other respiratory activities like coughing or sneezing, where particles may have higher release velocities. Understanding how local exhaust systems effectively capture and remove these particles is crucial for infection control. Moreover, the findings of the presented research may also apply to similar smaller indoor spaces and typical heat loads, as studied. However, future research should also explore larger spaces like auditoriums, gyms, large meeting rooms, etc., as well as other non-typical heat gains. These conditions may yield different experimental findings compared to this study's results. Furthermore, the results of the present study are considered reliable due to their evaluation at the steady state, thus experiments were not repeated. However, this approach could be a potential limitation for experimental studies, particularly for time-based analysis and more dynamic settings.

## 5. Conclusions

In this study, the effectiveness of local exhaust systems in mitigating exhaled pollutants in a mock-up meeting room is evaluated. A combination of local exhausts with traditional air distribution methods like mixing and displacement ventilation is examined. The aim was to enhance contaminant removal efficiency. The main findings are summarized as follows:

- (1) Local exhaust systems with displacement air distribution remained more effective as compared to mixing. With displacement air distribution, it enhanced the local air quality ( $\epsilon_p$ ) near the infector by up to 35% and improved ventilation effectiveness ( $\epsilon_v^b$ ) in the meeting room's entire breathing zone by a maximum of 25%.
- (2) The addition of a table plenum increased  $\epsilon_v^b$  up to 15% compared to configurations without it. Additionally, it improved local air quality, particularly for occupants farther from the displacement air supply inlet.

- (3) The number of operational local exhaust points directly impacts air quality with displacement ventilation. However, in the mixing system, an operational local exhaust with the infector reduces the importance of other exhaust points. In real scenarios, where the infector is often unknown or asymptomatic, it is advisable to utilize all available local exhaust points to maintain optimal air quality.

**Author Contributions:** Conceptualization, R.K. and M.F.E.; methodology, S.K., P.M. and M.F.E.; investigation, M.F.E.; resources, S.K. and P.M.; data curation, M.F.E.; writing—original draft preparation, M.F.E. and W.Z.; writing—review and editing, R.K., S.K. and P.M.; visualization, M.F.E. and W.Z.; supervision, R.K. All authors have read and agreed to the published version of the manuscript.

**Funding:** The Higher Education Commission (HEC), Pakistan, extended a personal grant (HRD/OSS-III/2022/HEC/118) to Muhammad Farhan Ejaz for this investigation.

**Data Availability Statement:** The raw data supporting the conclusions of this article will be made available by the authors on request. The data are not publicly available due to privacy.

**Acknowledgments:** The study was conducted at Aalto University, Finland, with generous material support from the university. The authors express their gratitude to Petteri Kivivuori for his efforts in constructing the experimental setup for this investigation. Special thanks are also conveyed to Afzaal Ather for his valuable assistance and contributions to this article.

**Conflicts of Interest:** Author Panu Mustakallio was employed by the company Halton Oy. The remaining authors declare that the research was conducted in the absence of any commercial or financial relationships that could be construed as a potential conflict of interest.

## References

1. Su, R.; Obrenovic, B.; Du, J.; Godinic, D.; Khudaykulov, A. COVID-19 Pandemic Implications for Corporate Sustainability and Society: A Literature Review. *Int. J. Environ. Res. Public Health* **2022**, *19*, 1592. [CrossRef] [PubMed]
2. Chinazzi, M.; Davis, J.T.; Ajelli, M.; Gioannini, C.; Litvinova, M.; Merler, S.; Piontti, Y.; Pastore, A.; Mu, K.; Rossi, L.; et al. The effect of travel restrictions on the spread of the 2019 novel coronavirus (COVID-19) outbreak. *Science* **2020**, *368*, 395–400. [CrossRef] [PubMed]
3. Brooks, S.K.; Webster, R.K.; Smith, L.E.; Woodland, L.; Wessely, S.; Greenberg, N.; Rubin, G.J. The psychological impact of quarantine and how to reduce it: A Rapid review of the evidence. *Lancet* **2020**, *395*, 912–920. [CrossRef] [PubMed]
4. WHO. *Considerations for Implementing and Adjusting Public Health and Social Measures in the Context of COVID-19: Interim Guidance*; WHO: Geneva, Switzerland, 2023.
5. Sheikhejad, Y.; Aghamolaei, R.; Fallahpour, M.; Motamedi, H.; Moshfeghi, M.; Mirzaei, P.A.; Bordbar, H. Airborne and aerosol pathogen transmission modeling of respiratory events in buildings: An overview of computational fluid dynamics. *Sustain. Cities Soc.* **2022**, *79*, 103704. [CrossRef] [PubMed]
6. Rabaan, A.A.; Al-Ahmed, S.H.; Al-Malkey, M.; Alsubki, R.; Ezzikouri, S.; Al-Hababi, F.H.; Sah, R.; Al Mutair, A.; Alhumaid, S.; Al-Tawfiq, J.A.; et al. Airborne transmission of SARS-CoV-2 is the dominant route of transmission: Droplets and aerosols. *Infect. Med.* **2022**, *29*, 10–19.
7. Morawska, L.; Bahnfleth, W.; Bluyssen, P.M.; Boerstra, A.; Buonanno, G.; Dancer, S.J.; Floto, A.; Franchimon, F.; Haworth, C.; Hogeling, J.; et al. Coronavirus Disease 2019 and Airborne Transmission: Science Rejected, Lives Lost. Can Society Do Better? *Clin. Infect. Dis.* **2023**, *76*, 1854–1859. [CrossRef] [PubMed]
8. Morawska, L.; Cao, J. Airborne transmission of SARS-CoV-2: The world should face the reality. *Environ. Int.* **2020**, *139*, 105730. [CrossRef] [PubMed]
9. Baboli, Z.; Neisi, N.; Babaei, A.A.; Ahmadi, M.; Sorooshian, A.; Birgani, Y.T.; Goudarzi, G. On the airborne transmission of SARS-CoV-2 and relationship with indoor conditions at a hospital. *Atmos. Environ.* **2021**, *261*, 118563. [CrossRef] [PubMed]
10. Robotto, A.; Civra, A.; Quaglino, P.; Polato, D.; Brizio, E.; Lembo, D. SARS-CoV-2 airborne transmission: A validated sampling and analytical method. *Environ. Res.* **2021**, *200*, 111783. [CrossRef]
11. Nazaroff, W.W. Indoor aerosol science aspects of SARS-CoV-2 transmission. *Indoor Air* **2022**, *32*, e12970. [CrossRef]
12. Scientific Brief: SARS-CoV-2 Transmission. Available online: <https://www.cdc.gov/coronavirus/2019-ncov/science/science-briefs/sars-cov-2-transmission.html#> (accessed on 7 May 2021).
13. Tang, S.; Mao, Y.; Jones, R.M.; Tan, Q.; Ji, J.S.; Li, N.; Shen, J.; Lv, Y.; Pan, L.; Ding, P.; et al. Aerosol transmission of SARS-CoV-2? Evidence, prevention and control. *Environ. Int.* **2020**, *144*, 106039. [CrossRef]
14. Xu, S.; Zhang, G.; Liu, X.; Li, X. CFD modelling of infection control in indoor environments: A focus on room-level air recirculation systems. *Energy Build.* **2023**, *288*, 113033. [CrossRef]
15. Diep, F. The 5 biggest lessons we’ve learned about how coronavirus spreads on campus. In *The Chronicle of Higher Education*; NASPA: Washington, DC, USA, 2020; Volume 3.



16. Shen, J.; Kong, M.; Dong, B.; Birnkrant, M.J.; Zhang, J. Airborne transmission of SARS-CoV-2 in indoor environments: A comprehensive review. *Sci. Technol. Built Environ.* **2021**, *27*, 1331–1367. [\[CrossRef\]](#)
17. Qian, H.; Zheng, X. Ventilation control for airborne transmission of human exhaled bio-aerosols in buildings. *J. Thorac. Dis.* **2018**, *10*, S2295–S2304. [\[CrossRef\]](#)
18. Li, Y.; Leung, G.M.; Tang, J.W.; Yang, X.; Chao, C.Y.H.; Lin, J.Z.; Lu, J.W.; Nielsen, P.V.; Niu, J.; Qian, H.; et al. Role of ventilation in airborne transmission of infectious agents in the built environment? A multidisciplinary systematic review. *Indoor Air* **2007**, *17*, 2–18. [\[CrossRef\]](#)
19. REHVA. REHVA COVID-19 Guidance Document: How to Operate HVAC and Other Building Service Systems to Prevent the Spread of the Coronavirus (SARS-CoV-2) Disease (COVID-19) in Workplaces. In *Federation of European Heating, Ventilation and Air Conditioning Associations (REHVA)*; REHVA: Ixelles, Belgium, 2021; Volume 3, Available online: [https://www.rehva.eu/fileadmin/user\\_upload/REHVA\\_COVID-19\\_guidance\\_document\\_V4.1\\_15042021.pdf](https://www.rehva.eu/fileadmin/user_upload/REHVA_COVID-19_guidance_document_V4.1_15042021.pdf) (accessed on 1 March 2024).
20. Zhao, X.; Liu, S.; Yin, Y.; Zhang, T.; Chen, Q. Airborne transmission of COVID-19 virus in enclosed spaces: An overview of research methods. *Indoor Air* **2022**, *32*, e13056. [\[CrossRef\]](#) [\[PubMed\]](#)
21. Kurnitski, J.; Kiil, M.; Mikola, A.; Vösa, K.-V.; Aganovic, A.; Schild, P.; Seppänen, O. Post-COVID ventilation design: Infection risk-based target ventilation rates and point source ventilation effectiveness. *Energy Build.* **2023**, *296*, 113386. [\[CrossRef\]](#)
22. Hirnikel, D.J. Validation of a CFD model for temperature and particulate concentration in a test room with mixed air and displacement ventilation/Discussion. *ASHRAE Trans.* **2003**, *109*, 80.
23. Liu, S.; Koupriyanov, M.; Paskaruk, D.; Fediuk, G.; Chen, Q. Investigation of airborne particle exposure in an office with mixing and displacement ventilation. *Sustain. Cities Soc.* **2022**, *79*, 103718. [\[CrossRef\]](#)
24. Barbosa, B.P.P.; de Carvalho Lobo Brum, N. Ventilation mode performance against airborne respiratory infections in small office spaces: Limits and rational improvements for COVID-19. *J. Braz. Soc. Mech. Sci. Eng.* **2021**, *43*, 316. [\[CrossRef\]](#)
25. Bhagat, R.K.; Wykes, M.D.; Dalziel, S.B.; Linden, P. Effects of ventilation on the indoor spread of COVID-19. *J. Fluid Mech.* **2020**, *903*, F1. [\[CrossRef\]](#)
26. Yin, Y.; Xu, W.; Gupta, J.K.; Guity, A.; Marmion, P.; Manning, A.; Gulick, B.; Zhang, X.; Chen, Q. Experimental study on displacement and mixing ventilation systems for a patient ward. *HVAC&R Res.* **2009**, *15*, 1175–1191.
27. Tian, X.; Li, B.; Ma, Y.; Liu, D.; Li, Y.; Cheng, Y. Experimental study of local thermal comfort and ventilation performance for mixing, displacement and stratum ventilation in an office. *Sustain. Cities Soc.* **2019**, *50*, 101630. [\[CrossRef\]](#)
28. Nielsen, P.V.; Li, Y.; Buus, M.; Winther, F.V. Risk of cross-infection in a hospital ward with downward ventilation. *J. Affect. Disord.* **2010**, *45*, 2008–2014. [\[CrossRef\]](#)
29. Zhang, C.; Nielsen, P.V.; Liu, L.; Sigmer, E.T.; Mikkelsen, S.G.; Jensen, R.L. The source control effect of personal protection equipment and physical barrier on short-range airborne transmission. *J. Affect. Disord.* **2022**, *211*, 108751. [\[CrossRef\]](#)
30. Su, W.; Yang, B.; Melikov, A.; Liang, C.; Lu, Y.; Wang, F.; Li, A.; Lin, Z.; Li, X.; Cao, G.; et al. Infection probability under different air distribution patterns. *J. Affect. Disord.* **2022**, *207*, 108555. [\[CrossRef\]](#)
31. Danca, P.; Coşoiu, C.I.; Nastase, I.; Bode, F.; Georgescu, M.R. Personalized Ventilation as a Possible Strategy for Reducing Airborne Infectious Disease Transmission on Commercial Aircraft. *Appl. Sci.* **2022**, *12*, 2088. [\[CrossRef\]](#)
32. Lu, Y.; Oladokun, M.; Lin, Z. Reducing the exposure risk in hospital wards by applying stratum ventilation system. *J. Affect. Disord.* **2020**, *183*, 107204. [\[CrossRef\]](#)
33. Qin, C.; Zhang, S.-Z.; Li, Z.-T.; Wen, C.-Y.; Lu, W.-Z. Transmission mitigation of COVID-19: Exhaled contaminants removal and energy saving in densely occupied space by impinging jet ventilation. *J. Affect. Disord.* **2023**, *232*, 110066. [\[CrossRef\]](#)
34. Cheong, C.H.; Park, B.; Ryu, S.R. Effect of under-floor air distribution system to prevent the spread of airborne pathogens in classrooms. *Case Stud. Therm. Eng.* **2021**, *28*, 101641. [\[CrossRef\]](#)
35. Morawska, L.; Tang, J.W.; Bahnfleth, W.; Bluyssen, P.M.; Boerstra, A.; Buonanno, G.; Cao, J.; Dancer, S.; Floto, A.; Franchimon, F.; et al. How can airborne transmission of COVID-19 indoors be minimised? *Environ. Int.* **2020**, *142*, 105832. [\[CrossRef\]](#) [\[PubMed\]](#)
36. Curtius, J.; Granzin, M.; Schrod, J. Testing mobile air purifiers in a school classroom: Reducing the airborne transmission risk for SARS-CoV-2. *Aerosol Sci. Technol.* **2021**, *55*, 586–599. [\[CrossRef\]](#)
37. Sheraz, M.; Mir, K.A.; Anus, A.; Kim, S.; Lee, W.R. SARS-CoV-2 airborne transmission: A review of risk factors and possible preventative measures using air purifiers. *Environ. Sci. Process. Impacts* **2022**, *24*, 2191–2216. [\[CrossRef\]](#) [\[PubMed\]](#)
38. Zhao, B.; Liu, Y.; Chen, C. Air purifiers: A supplementary measure to remove airborne SARS-CoV-2. *J. Affect. Disord.* **2020**, *177*, 106918. [\[CrossRef\]](#)
39. Ng, Y.; Li, Z.; Chua, Y.X.; Chaw, W.L.; Zhao, Z.; Er, B.; Pung, R.; Chiew, C.J.; Lye, D.C.; Heng, D.; et al. Evaluation of the Effectiveness of Surveillance and Containment Measures for the First 100 Patients with COVID-19 in Singapore—January 2–February 29, 2020. *MMWR. Morb. Mortal. Wkly. Rep.* **2020**, *69*, 307–311. [\[CrossRef\]](#) [\[PubMed\]](#)
40. Bivolarova, M.P.; Melikov, A.K.; Mizutani, C.; Kajiwar, K.; Bolashikov, Z.D. Bed-integrated local exhaust ventilation system combined with local air cleaning for improved IAQ in hospital patient rooms. *J. Affect. Disord.* **2016**, *100*, 10–18. [\[CrossRef\]](#)
41. Dygert, R.K.; Dang, T.Q. Mitigation of cross-contamination in an aircraft cabin via localized exhaust. *J. Affect. Disord.* **2010**, *45*, 2015–2026. [\[CrossRef\]](#)
42. Dygert, R.K.; Dang, T.Q. Experimental validation of local exhaust strategies for improved IAQ in aircraft cabins. *J. Affect. Disord.* **2012**, *47*, 76–88. [\[CrossRef\]](#)

43. Yang, J.; Sekhar, C.; Cheong, D.K.; Raphael, B. A time-based analysis of the personalized exhaust system for airborne infection control in healthcare settings. *Sci. Technol. Built Environ.* **2015**, *21*, 172–178. [\[CrossRef\]](#)
44. Olmedo, I.; Sánchez-Jiménez, J.; Peci, F.; de Adana, M.R. Personal exposure to exhaled contaminants in the near environment of a patient using a personalized exhaust system. *J. Affect. Disord.* **2022**, *223*, 109497. [\[CrossRef\]](#)
45. Liu, W.; Liu, L.; Xu, C.; Fu, L.; Wang, Y.; Nielsen, P.V.; Zhang, C. Exploring the potentials of personalized ventilation in mitigating airborne infection risk for two closely ranged occupants with different risk assessment models. *Energy Build.* **2021**, *253*, 111531. [\[CrossRef\]](#) [\[PubMed\]](#)
46. Yang, J.; Sekhar, S.C.; Cheong, K.W.D.; Raphael, B. Performance evaluation of a novel personalized ventilation-personalized exhaust system for airborne infection control. *Indoor Air* **2015**, *25*, 176–187. [\[CrossRef\]](#) [\[PubMed\]](#)
47. Ju, J.T.; Boisvert, L.N.; Zuo, Y.Y. Face masks against COVID-19: Standards, efficacy, testing and decontamination methods. *Adv. Colloid Interface Sci.* **2021**, *292*, 102435. [\[CrossRef\]](#) [\[PubMed\]](#)
48. Brienens, N.C.J.; Timen, A.; Wallinga, J.; Van Steenberghe, J.E.; Teunis, P.F.M. The Effect of Mask Use on the Spread of Influenza during a Pandemic. *Risk Anal.* **2010**, *30*, 1210–1218. [\[CrossRef\]](#) [\[PubMed\]](#)
49. Fischer, E.P.; Fischer, M.C.; Grass, D.; Henrion, I.; Warren, W.S.; Westman, E. Low-cost measurement of face mask efficacy for filtering expelled droplets during speech. *Sci. Adv.* **2020**, *6*, eabd3083. [\[CrossRef\]](#)
50. Saunders-Hastings, P.; Crispo, J.A.; Sikora, L.; Krewski, D. Effectiveness of personal protective measures in reducing pandemic influenza transmission: A systematic review and meta-analysis. *Epidemics* **2017**, *20*, 1–20. [\[CrossRef\]](#) [\[PubMed\]](#)
51. Matuschek, C.; Moll, F.; Fangerau, H.; Fischer, J.C.; Zänker, K.; van Griensven, M.; Schneider, M.; Kindgen-Milles, D.; Knoefel, W.T.; Lichtenberg, A.; et al. The history and value of face masks. *Eur. J. Med. Res.* **2020**, *25*, 1–6. [\[CrossRef\]](#)
52. Ahmad, F.; Wahab, S.; Ahmad, F.A.; Alam, M.I.; Ather, H.; Siddiqua, A.; Ashraf, S.A.; Abu Shaphe, M.; Khan, M.I.; Beg, R.A. A novel perspective approach to explore pros and cons of face mask in prevention the spread of SARS-CoV-2 and other pathogens. *Saudi Pharm. J.* **2021**, *29*, 121–133. [\[CrossRef\]](#)
53. Matuschek, C.; Moll, F.; Fangerau, H.; Fischer, J.C.; Zänker, K.; van Griensven, M.; Schneider, M.; Kindgen-Milles, D.; Knoefel, W.T.; Lichtenberg, A.; et al. Face masks: Benefits and risks during the COVID-19 crisis. *Eur. J. Med. Res.* **2020**, *25*, 1–8. [\[CrossRef\]](#)
54. Shen, J.; Kong, M.; Dong, B.; Birnkrant, M.J.; Zhang, J. A systematic approach to estimating the effectiveness of multi-scale IAQ strategies for reducing the risk of airborne infection of SARS-CoV-2. *J. Affect. Disord.* **2021**, *200*, 107926. [\[CrossRef\]](#)
55. Geiss, O. Effect of Wearing Face Masks on the Carbon Dioxide Concentration in the Breathing Zone. *Aerosol Air Qual. Res.* **2021**, *21*, 200403. [\[CrossRef\]](#)
56. Patel, S.; Majmundar, S. Physiology, Carbon Dioxide Retention. In *StatPearls*; StatPearls Publishing: Treasure Island, FL, USA. Available online: <https://pubmed.ncbi.nlm.nih.gov/29494063/> (accessed on 1 March 2024).
57. Suen, L.; Guo, Y.; Ho, S.; Au-Yeung, C.; Lam, S. Comparing mask fit and usability of traditional and nanofibre N95 filtering facepiece respirators before and after nursing procedures. *J. Hosp. Infect.* **2020**, *104*, 336–343. [\[CrossRef\]](#) [\[PubMed\]](#)
58. Pleil, J.D.; Wallace, M.A.G.; Davis, M.D.; Matty, C.M. The physics of human breathing: Flow, timing, volume, and pressure parameters for normal, on-demand, and ventilator respiration. *J. Breath Res.* **2021**, *15*, 042002. [\[CrossRef\]](#) [\[PubMed\]](#)
59. Laporthe, S.; Virgone, J.; Castanet, S. A comparative study of two tracer gases: SF<sub>6</sub> and N<sub>2</sub>O. *J. Affect. Disord.* **2001**, *36*, 313–320. [\[CrossRef\]](#)
60. Wu, Y.; Tung, T.C.; Niu, J.-L. On-site measurement of tracer gas transmission between horizontal adjacent flats in residential building and cross-infection risk assessment. *J. Affect. Disord.* **2016**, *99*, 13–21. [\[CrossRef\]](#) [\[PubMed\]](#)
61. Zhao, W.; Lestinen, S.; Kilpeläinen, S.; Yuan, X.; Jokisalo, J.; Kosonen, R.; Guo, M. Exploring the potential to mitigate airborne transmission risks with convective and radiant cooling systems in an office. *J. Affect. Disord.* **2023**, *245*, 110936. [\[CrossRef\]](#)
62. Mundt, M.; Mathisen, H.M.; Moser, M.; Nielsen, P.V. *Ventilation Effectiveness: Rehva Guidebooks*; Rehva Guidebook, no. 2; Federation of European Heating and Ventilation Association: Brussels, Belgium, 2004.
63. Zhou, Q.; Qian, H.; Ren, H.; Li, Y.; Nielsen, P.V. The lock-up phenomenon of exhaled flow in a stable thermally-stratified indoor environment. *J. Affect. Disord.* **2017**, *116*, 246–256. [\[CrossRef\]](#)
64. Flynn, M.R.; Ellenbecker, M.J. Capture Efficiency of Flanged Circular Local Exhaust Hoods. *Ann. Occup. Hyg.* **1986**, *30*, 497–513. [\[CrossRef\]](#)
65. Huang, R.F.; Chen, J.L.; Chen, Y.-K.; Chen, C.-C.; Yeh, W.-Y.; Chen, C.-W. The Capture Envelope of a Flanged Circular Hood in Cross Drafts. *Am. Ind. Hyg. Assoc. J.* **2001**, *62*, 199–207. [\[CrossRef\]](#)
66. Cheong, K.; Phua, S. Development of ventilation design strategy for effective removal of pollutant in the isolation room of a hospital. *J. Affect. Disord.* **2006**, *41*, 1161–1170. [\[CrossRef\]](#)
67. Ai, Z.; Mak, C.M.; Gao, N.; Niu, J. Tracer gas is a suitable surrogate of exhaled droplet nuclei for studying airborne transmission in the built environment. *Build. Simul.* **2020**, *13*, 489–496. [\[CrossRef\]](#) [\[PubMed\]](#)

**Disclaimer/Publisher’s Note:** The statements, opinions and data contained in all publications are solely those of the individual author(s) and contributor(s) and not of MDPI and/or the editor(s). MDPI and/or the editor(s) disclaim responsibility for any injury to people or property resulting from any ideas, methods, instructions or products referred to in the content.